

Imaging Techniques in Critical Care Nephrology

CHAPTER 33

Ultrasonography and Doppler Techniques

Mario Meola and Ilaria Petrucci

OBJECTIVES

This chapter will:

1. Highlight advantages and theoretical outlines, preliminary to practice of ultrasound (US) in clinical work-up of acute kidney injury (AKI)
2. Summarize US morphological and functional parameters used in clinical diagnosis of AKI
3. Report patterns and features supporting US diagnosis of volume overload and various forms of AKI.

Advances in digital technology have improved the ability of ultrasound (US) to characterize tissue damage. Nevertheless, US is not sufficient to define the nature of acute kidney injury (AKI). Echo-signals from tissues and vessels can be analyzed and represented in different ways. Gray-scale US or B-Mode represents structural echoes as brightness points. Color Doppler (CD) represents changes in blood flow-velocity using spectral analysis or colorimetric scale. Contrast-enhanced ultrasound (CEUS) analyzes the vascular enhancement after intravenous infusion of a low mechanical index amplifier. Elastosonography analyzes tissues deformation and represents the degree of stiffness. Potentially, all these applications can characterize parenchymal damage. In fact, the road ahead is still arduous. B-Mode parameters (renal diameter, thickness and parenchymal echogenicity, urinary tract status) provide a correct framework of AKI only in 50-70% of cases.¹ CD provides only indirect information about the nature of damage by analysing microvascular hemodynamics. CEUS indications in AKI are not specific and elastosonography of native kidneys is limited by the organ depth. So, US is not always able to define the nature of renal damage, although it remains a first-line technique, safe and useful for evaluating patients with AKI, in order to exclude urinary tract obstruction or a chronic disease and to guide clinical workup.

DEFINITION OF ACUTE KIDNEY INJURY

AKI is defined as a reduction in renal function within 48 hours based on an elevation in serum creatinine (sCr) level, a reduction in urine output, the need for renal replacement therapy (RRT), or a combination of these conditions. Causes of AKI are divided into prerenal, renal, and postrenal. Near 70% of cases of AKI are caused by a sudden reduction in renal perfusion. Persistent hypotension and shock are common causes of *prerenal AKI*. In all these conditions, renal parenchyma integrity is preserved and glomerular filtration rate (GFR) rapidly recovers by restoring renal perfusion rate. *Parenchymal AKI* derives from drugs, toxics, and glomerular, interstitial, and vascular diseases. Acute tubular necrosis (ATN) results from prolonged hypotension or toxic effects of drugs, heavy metals, iodinated contrast, or tubular obstruction. In critical care unit major surgery, multiorgan failure syndrome, and septicemia are the most common causes of AKI. *Postrenal AKI* results from urinary tract obstruction of the ureter (lithiasis, clots, tumors, etc.) or of the lower urinary tract (bladder and prostate diseases, urethral obstructions). AKI is reversible when the obstruction is removed.²

PATHOGENESIS OF ACUTE DAMAGE AND ROLE OF MICROCIRCULATION

Processes leading to tubular damage and renal dysfunction follow a final common pathway, i.e. a diffuse or partial renal ischemia, whatever the nature of injury. In AKI early stages, a severe vasoconstriction occurs with a reduced sensitivity to vasodilation. These two factors reduce the availability of oxygen/nutrients, leading to tubular damage. Vascular networks mostly exposed to vasoconstriction and endothelial damage are preglomerular and outer renal medulla vessels. The earliest changes in proximal tubular cells are loss of polarity, relocation of Na⁺/K⁺ ATPase pumps,

and disarrangement of tight-junctions and cytoskeleton. These events favour apoptosis, necrosis, and epithelial cell barrier collapse, resulting in the filtrate back-leak. Therefore, dead cells sloughed into the tubular lumen aggregate with debris and tubular proteins leading to cast formation and lumen obstruction. The increase of intratubular pressure underlies GFR fall and filtrate back-leak into the interstitium.³

ROLE OF ULTRASOUND IN CLINICAL WORKUP

The assessment of AKI is not always easy but it is essential in clinical workup. In fact, presentation, clinical course, treatment, and prognosis depend on damage severity, duration of GFR impairment, presence/absence of complications, and pre-existent diseases.⁴

US is the first-choice imaging procedure in AKI, simple to use, well tolerated, and easy to access by nephrologists and intensivists, even at bedside. B-Mode should evaluate *kidney morphological parameters* (longitudinal diameter, parenchymal thickness, echogenicity of cortico-medullary boundary, renal profiles, central hyperechoic complex, and urinary tract), *signs of volume overload* (pleural and pericardial effusion, ascites, peripheral oedema) and *signs of increased central venous pressure* (inferior vena cava-IVC and hepatic veins-HV dynamic). Renal morphology distinguishes AKI from chronic kidney disease (CKD) where kidneys are shrunk and reduced in size.⁵ On the contrary, an enlarged kidney with rounded and hypoechoic pyramids and hyperechoic cortex in a patient with a sudden fall of GFR suggests an acute glomerular disease with crescents, an acute interstitial nephropathy (AIN), an ATN, or an infiltrative disease.⁶ Kidney size also increases in renal vein thrombosis and acute rejection.⁷ Renal echogenicity is strictly related to histology and to the number and geometric arrangement of cortex and medullar interfaces. Anisotropic interfaces of cortical boundary are more echoic if compared to regular and isotropic structures of renal medulla. Instead, the parenchymal ring shows a hypoechoic texture if compared to the liver and spleen, and it is clearly distinguishable from the hyperechoic central complex. The parenchymal boundary is hypoechoic when interstitial oedema lowers the scattering level. Conversely, the cortex or medulla become hyperechoic when the scattering level increases compared to the surrounding tissues due to inflammatory cell infiltration. However, many factors may affect kidney texture, so this parameter is not specific.

Parenchymal thickness is a differential criterion between AKI and CKD. In chronic disease thickness and kidney size are evenly reduced (chronic glomerulonephritis or AIN) or irregular (pyelonephritis, obstructive uropathy). Bilateral nephromegaly, increase of parenchymal thickness, widespread hypoechogenicity, and disarrangement of pyramids suggest a rapidly progressive glomerulonephritis, ATN, AIN, and sepsis.⁵ B-Mode is the most reliable imaging to rule out damage due to acute urinary tract obstruction. In transplant, US sensitivity is very high (>90%) whereas specificity is very high only in severe hydronephrosis.⁵

CD mapping of renal vessels rules out arterial and venous thrombo-embolism and provides a full picture of renal perfusion. Doppler spectral analysis provides quantitative data on velocity profile and intrarenal resistances. In AKI early phases, vasoconstriction and interstitial oedema increase flow resistance modifying spectral tracing. The

low-resistance pattern is replaced by a monophasic pulsatile trace where discontinuous flow becomes prevalent. In renal vein thrombosis (RVT), spectral tracing becomes triphasic and shows a reverse wave, like in hemolytic-uremic syndrome (HUS) and in renal cortical necrosis. Intrarenal resistive indexes [(resistive index (RI), pulsatility index (PI)] provide a semiquantitative marker of microvascular hemodynamic during damage and recovery phases of AKI. It is advisable to standardize RI measurements as the average of three values in an interlobar artery close to the mesorenal column. Unfortunately, several factors can influence RIs, particularly in uncooperative or unstable patients with severe cardio-pulmonary illness or after major surgery.⁸

Usually, RI is normal or reduced in prerenal AKI while it rapidly increases when a persistent vasoconstriction leads to tubular damage. In AIN, RIs are higher than in the acute glomerular disease (0.75 vs. 0.58)⁹ and are even higher in patients with ATN, vasculitis, or hepato-renal syndrome (HRS) (>0.78-0.82). RI is a reliable marker of AKI after coronary bypass, shock, trauma, or sepsis. In all these conditions, if RI basal values are normal (<0.68), patients do not develop AKI. Conversely, when baselines RI are >0.77-0.78, patients develop an acute dysfunction requiring RRT within 1-5 days. Available data suggest that a progressive reduction of RI towards values according to a low-resistance blood-flow is predictive of kidney recovery.

CEUS could play a decisive role in diagnostic workup monitoring hemodynamic changes in regional renal flow. Parameters such as perfusion velocity, regional blood-flow and wash-in/wash-out curves should be very useful despite the lack of standard operating procedures and evidence.

PRERENAL ACUTE KIDNEY INJURY

Prerenal AKI is a functional framework and regresses in 24 to 48 hours with proper treatment; alternatively, it may evolve to ATN if ischemia persists. Many forms of prerenal AKI are intersections between cardiovascular and kidney disease. *Cardiorenal syndrome (CRS)* describes the complex inter-relationships between acute or chronic heart and kidney diseases. US provides a significant contribution in CRS type 1, where AKI is associated with acute heart failure (AHF) and in CRS type 2, where AKI accompanies chronic heart failure (CHF).¹⁰

Acute Kidney Injury Due to Acute Heart Failure

In *left AHF*, the sudden drop in ejection fraction (EF) reduces visceral perfusion favouring vasoconstriction and blood-flow redistribution. In kidneys, flow redistribution and activation of the angiotensin-renin system lead to sodium/water retention. Pathophysiology of this adaptive mechanism is quantitatively different in AHF and CHF. *Right and biventricular AHF* result in fluid retention in the systemic venous circulation. Signs of right overload are cyanosis, distended jugular veins, hepato-splenomegaly, pleural and pericardial effusions, and peripheral oedema.

In AHF with reduction of EF, US does not show specific signs. In the absence of a preexisting organ disease, kidneys appear normal. Cortico-medullary texture may be normal or hyperechoic if preglomerular vasoconstriction and hypoperfusion are persistent. There is no urinary stasis and the bladder is empty. Initially, RIs are very low due to vasodilation induced by intrarenal autoregulation mechanisms. Afterwards, if ischemia is persistent, they increase

very rapidly whereas functional impairment progresses toward ATN. IVC collaps and HV are very thin. Absence of systemic congestion persists as long as left AHF does not become biventricular failure. In patients complaining AHF, the subxiphoid four-chamber view using the convex abdominal probe shows an adaptive remodelling of the heart, such as a concentric, symmetrical, or asymmetrical left ventricle hypertrophy (LVI) or a change in heart volume.

Lung Comet Tails

Air in the pulmonary alveoli generates different artifacts. Basic semiotics of lung is founded on the interpretation of these artifacts. Lung and pleural layers are indistinguishable at US and they form a single interface, the pleural line, which moves under the ribs during the breath. This movement, called *lung sliding* or *gliding*, at M-Mode appears as an undulating line (*seashore sign*). In intercostal scans, pleuro-pulmonar interface generates a strong echo-signal that bounces back and forth between transducer and pleural line several times, producing many reverberations called *A-Lines*. These appear as thin horizontal hyperechoic lines repeating at symmetrical distance from the surface to the depth.

Similarly, oedema or fibrosis of the subpleural septa generates some reflective interfaces. Ringing of pulses within these strong reflectors generates distal reverberations (*B-Lines* or *comet tail sign*). B-Lines have the same meaning of *Kerley B-lines* in traditional radiograms.¹⁰ Usually, at US, comets appear as laser-like vertical hyperechoic beams arising from the pleural line and synchronously moving with the lung sliding in depth (Fig. 33.1). Alveolar-Interstitial congestion is mild if comets are spaced from each other by at least 7 mm. In cardiogenic oedema their number correlates with the severity of the dyspnea and they follow a symmetric distribution, progressing from the lateral and inferior spaces to the anterior upper chest areas. Lung comets are also evident in different clinical frameworks such as diffuse interstitial diseases, pulmonary fibrosis, acute respiratory distress syndrome, interstitial or lobar pneumonia, and pulmonary laceration. All that significantly reduces sign specificity. Comet tails can be highlighted with any type

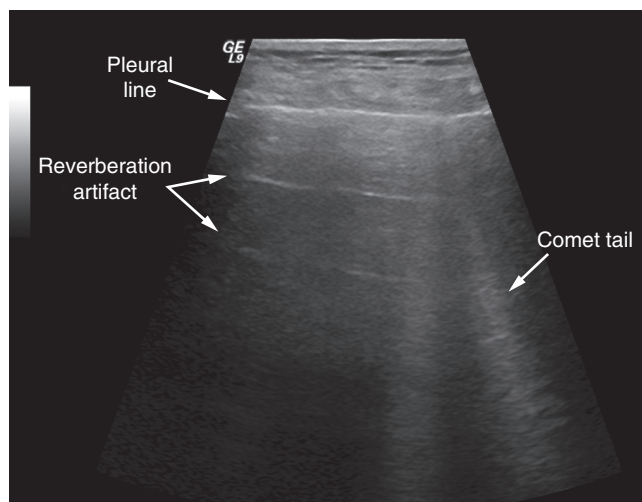


FIGURE 33.1 Comet-tail artifact. This reverberation artifact corresponds to kerley B striae and it is generated by the intense US beam reflection in hyperhydrated subpleural septa.

of probe and in any patient position. They have to be countered in the whole chest from the lateral and inferior to the anterior upper chest areas, on the right and left hemithorax. The most employed scanning technique is the eight-zone examination, where four chest areas per each hemithorax, from second to fourth intercostal space along the parasternal, mid-clavicular, anterior, and medium axillary lines, are scanned.¹¹ Sum of mean averages of comets in each point creates a semi-quantitative score of oedema.

Acute Kidney Injury Due to Chronic Heart Failure

CHF usually results from a systolic dysfunction that impairs contractility/ventricular emptying or diastolic dysfunction that impairs relaxation/ventricular filling. Systolic dysfunction is most commonly associated to myocardial infarction, whereas diastolic dysfunction is more frequent in diabetes, hypertension, and obesity. All forms of heart disease favour a structural/functional ventricle remodelling supported by neuro-hormonal stimuli in response to pressure/volume overload and/or cellular damage. Right CHF is often a complication of left ventricular failure.

US and CD imaging are very useful in the characterization of CHF. The long-axis subxiphoid four-chamber view using a convex probe allows nephrologists and intensivists to analyze cardiac morphology, generalized hypokinesis, right atrial dilation, LVH, and pericardial effusion. When return rate exceeds filling capacity of the right heart, central venous pressure increases. IVC and HV congestion increases liver volume. IVC antero-posterior diameter becomes ≥ 2 cm and does not vary with the breath. At US, the vein is stiff (Fig. 33.2), less squeezable under compression manoeuvres, and its collapsibility index is $<50\%$.¹² These data are useful parameters in the assessment of systemic overload.

Liver Stasis

In CHF, liver increases in volume due to congestion. Sagittal paramedian diameter of the right lobe exceeds 13 cm, profiles are rounded, and tissue texture is homogeneous. In early stages, texture is bright and hyperechoic due to steatosis.

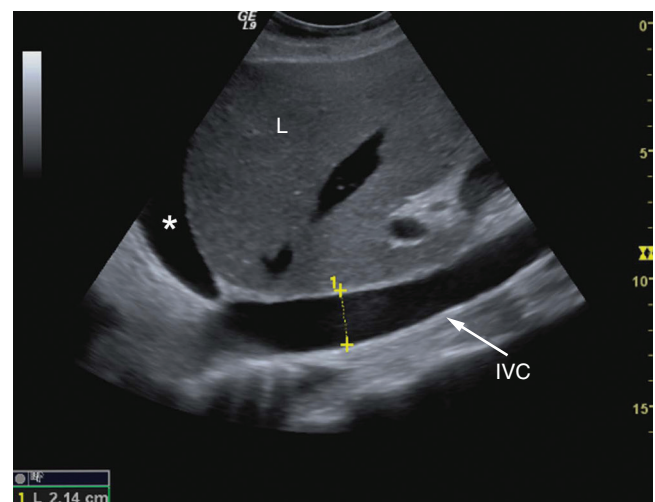


FIGURE 33.2 See also color plates. Right overload. When venous return exceeds the right heart capacity, central venous pressure increases and vena cava appears dilated (antero-posterior diameter >2 cm) and not collapsing.

In the late phases, persistent congestion of centrilobular sinusoids due to impairment of venous outflow favours hypoxia, death of hepatocytes until micronodular cirrhotic regeneration. Perisinusoidal fibrosis reduces HV elasticity, modifying the pattern of spectral trace. Normal triphasic trace becomes a flattened and monophasic curve without inflections. Whether tricuspid incontinence overlaps, flow may be reduced or reversed during ventricular systole until the curve becomes biphasic.¹

Pleural Effusion, Ascites, and Peripheral Oedema

In CHF, scan of the costo-phrenic angles on both sides should be performed to highlight the “curtain sign” (i.e., lung movement covering the liver or the spleen during inspiration). Frequently, these scans reveal a pleural effusion. Small effusions have to be found in the sitting position using sagittal and intercostal scans along the paravertebral and posterior axillary lines. Large effusions are also evident in supine decubitus. At gray-scale US, pleural effusion appear as an anechoic fluid collection between liver/diaphragm and pleuro-pulmonary interfaces. Lungs float in pleural fluid and appear normal or consolidated due to atelectasis. Placing an M-mode line across the effusion, a moving back and forth of the pleuro-pulmonary line from the chest wall becomes evident at breathing. Features of pleural effusions vary according to their nature and duration. Transudates are usually anechoic whereas echoic effusions could be either transudates or exudates. Effusions containing corpuscolated echoes (*plankton sign*) as well as those showing a complex septated or complex nonseptated echo-pattern are pleural exudates, empyema, or hemorrhage.

Small effusions in Morrison and/or Douglas pouch, pericardial, and perisplenic spaces indicate a systemic venous congestion. Spleen is usually normal, even if its vascular hilum is congested. Kidneys in B-Mode are globose-shaped, increased in volume, and diffusely hypoechoic due to fluid accumulation. At CD, renal veins are patent but spectral curve often shows a “W” like modulation similar to the one in IVC/HV, indicating a volume overload.¹

Central Venous Pressure and Hepatic Veins Spectral Tracing

HV spectral trace should be recorded in the middle HV during inspiration using subcostal scans in supine or left side decubitus. A volume sample should be placed near the confluence. Normal waveform is a ‘W’ triphasic trace with one positive and two negative peaks. The positive “a” peak coincides with atrial systole; ‘S’ and ‘D’ negative peaks correspond to ventricle systole and diastole. A transitional negative, neutral, or positive ‘v’ peak can be evident between ‘S’ and ‘D’ waves. The ‘a’ wave begins with the P wave at ECG and its peak corresponds to the beginning of the QRS complex. ‘S’ and ‘D’ waves follow the T wave at ECG. Mechanical ventilation, atrial fibrillation, or HV thrombosis are the most common causes of irregularity of waveform. In cirrhosis with portal hypertension and ascites, spectral wave is monophasic, continuous, and flattened.

Interpretation of HV velocity versus time curve (V/t curve) requires knowledge of heart physiology.¹³ Curve inflections are linked to atrial pressure variations transmitted towards IVC and HV. The ‘a’ wave represents the reversal flow into the liver during atrial systole. ‘S’ wave represents the rapid atrial filling during ventricular systole. Stretching of tricuspid annulus toward the cardiac apex during the

systole increases the flow rate from the liver to the heart. The ‘v’ wave indicates a low reversal flow during the return of cusps to their resting position. ‘D’ wave corresponds to rapid ventricular filling during the early diastole after the tricuspid valve opening.

In tricuspid regurgitation, during the rapid atrial filling, the blood flow is forced into the atrium. ‘S’ wave changes and it gradually becomes smaller than ‘D’ wave. In severe tricuspid regurgitation, ‘a’, ‘S’, and ‘v’ waves are all retrograde and fused into a single negative deflection alternating with an anterograde ‘D’ wave. Finally, HVs diagram becomes biphasic with a single retrograde ‘S’ wave and an anterograde ‘D’ wave. In CHF, spectral trace is similar to that of tricuspid regurgitation. In any case, ‘S’ wave never becomes retrograde in the absence of severe regurgitation. Generally, it is impossible to distinguish between mild tricuspid regurgitation and right-sided CHF because these entities commonly coexist. Lastly, HV waveforms in constrictive pericarditis or severe pericardial effusion are a variant of the triphasic curve that includes an extra retrograde wave at the end of diastole, between ‘D’ and ‘a’ waves, which is more evident during the expiratory phase (Fig. 33.3).

Hepato-Renal Syndrome

In cirrhosis and ascites, a latent prerenal AKI due to arterial hypotension, hypovolemic status, and decreased renal blood flow is evident.¹⁴ In this case, AKI may precipitate for gastrointestinal bleeding, sepsis, or toxics. In cirrhosis with refractory ascites, a prerenal, irreversible AKI may also develop. This form of AKI, named HRS, has an unknown pathogenesis but it is caused by a severe renal vasoconstriction with peripheral vasodilation. In HRS, tubular function is preserved and no proteinuria or histological damages are evident. There are two clinical variants of HRS: 1) Type 1 with a progressive kidney failure triggered by a spontaneous bacterial peritonitis; 2) Type 2 with a moderate and stable reduction in GFR occurs in patients with refractory ascites and relatively preserved hepatic function.

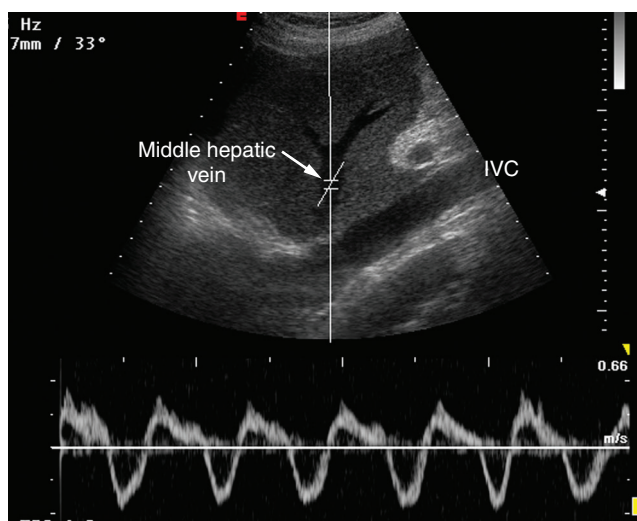


FIGURE 33.3 See also color plates. Venogram morphological patterns during pericarditis with severe effusion. Parasagittal scan on inferior vena cava. Cardiac filling is hindered because of severe effusion, so a biphasic wave appears together with a retrograde wave to the liver at the end of diastole. This wave becomes more prominent during the expiratory phase. IVC, inferior vena cava.

At US, HRS shows signs of decompensated cirrhosis associated with portal hypertension: the liver is reduced in volume and it loses its uniform smooth hepatic echotexture showing a micro- or macronodular pattern. HV are thin and irregular, while portal veins are dilated (>13 mm) with biphasic or reverse flow. In the late stages, recanalization of paraumbilical veins, portal-systemic collateral pathways, splenomegaly, and ascites can coexist. In the absence of preexisting damage, kidneys are normal and the echo-pattern of the corticomedullary boundary is preserved even though hypoechogenicity of the medulla may be present. Patients with HRS have very high values of RIs (0.79 ± 0.6). RI is an independent predictor of renal dysfunction and HRS in patients with chronic liver disease without renal insufficiency. Therefore, serial measurements of RI in patients with liver disease may select a subset of patients without GFR fall but at high risk for AKI and HRS. RI increase precedes the increase of sCr and it is a sign of reduced survival.

PARENCHYMAL ACUTE KIDNEY INJURY

Parenchymal Diseases

ATN, the most common form of AKI, results from a direct (toxics, drugs, iodinated contrast, sepsis) or indirect injury (ischemia, obstruction) of tubular epithelium. At US, kidneys are normal or globose-shaped and increased in volume; pyramids are prominent, hypoechoic, and disorganized. Volume enlargement and medullary hypoechogenicity change according to the severity of interstitial oedema and tubular damage. Cortex is normal and it can show a diffuse hyper-echogenicity only in ATN related to toxics.¹ Kidneys also appear enlarged and swollen in post-surgical AKI where the cortex is hyperechoic and the medulla is diffusely hypoechoic.¹ Morphological parameters and renal echotexture are nonspecific. However, microcirculation hemodynamic alterations are helpful in the clinical setting and follow-up.¹⁵ A rapid increase in intrarenal RIs anticipates sCr increase and directly correlates with it.¹ 80% of patients with prerenal AKI show a reduced V/t curve with low RI values. Conversely, 91% of patients with parenchymal AKI show a significant increase in RI values (>0.75), due to high parenchymal impedance.¹ In clinical studies, RI >0.79 are predictive of severe organic damage.¹⁶ In AKI recovery phase, RI improvement precedes sCr decreasing.¹

AIN due to NSAIDs and antimicrobials drugs is a frequent cause of AKI in the elderly. At B-Mode, as in ATN, kidney morphology is nonspecific. Increase in volume is associated with a widespread medullary hyper-echogenicity due to interstitial oedema and inflammatory infiltration, which increases volume unit scatterers (Fig. 33.4). In acute pyelonephritis, US is often normal. There may be focal hypo/hyperechoic areas depending on oedema, hemorrhage, and neutrophil infiltration. In some cases, a focal inflammatory area may produce a pseudo-mass effect on adjacent parenchymal areas. On the contrary, acute bacterial pyelonephritis with systemic infection may produce a diffuse kidney enlargement with hypo- or hyper-echogenicity, loss of cortico-medullary differentiation, and uro-epithelial thickening. Hemodynamic flow changes and CD features are related to damage severity and progression. In fact, in reversible AKI due to AIN, RI are commonly ≤ 0.70 due to blood redistribution in normo-functioning renal cortex.

Acute cortical necrosis (ACN) is a rare and irreversible type of AKI due to an arterial vasospasm caused by drugs,

microcirculation damage, or thrombosis. Necrosis can be focal, multifocal, or diffuse and may affect both kidneys. In most cases, medulla, juxta-medullary cortex, and a thin rhyme of sub-capsular cortex are spared. In ACN due to shock, sepsis, myocardial infarction, and burns, kidneys have a normal size without cortico-medullary differentiation and sometimes show a thin hypoechoic perirenal layer due to reactive oedema.¹ In ATN caused by intensive physical exercise and NSAIDs, hypoechoic wedge-shaped areas appear at CT but they become evident very late at US.

HUS is a rare disease characterized by hemolytic anemia, thrombocytopenia, and AKI due to bacterial endotoxins and severe endothelial damage of renal, brain, and intestinal capillaries and arterioles.¹ During the acute phase, kidneys are enlarged and hypoechoic, with RIs markedly increased that become normal after GFR recovery.

Vascular Diseases

In 50% of cases, renal infarction is caused by thromboembolism due to fibrillation, cardiomyopathy, or endocarditis.¹⁷ It can be focal, multifocal, or massive [27,28] [64,65] and affects elderly patients. It can occur also in young subjects without any thrombogenic risk. B-Mode is never diagnostic, but its sensitivity and specificity significantly increase with CD and CEUS. Segmental infarction appears as a triangular, non-vascularized hypoechoic area. CEUS improves the evaluation of small vessels, thus identifying focal or multi-focal ischemic areas. Diagnosis of main artery thrombosis is easy in renal transplant. At B-Mode, the kidney appears globular, increased in volume, hypoechoic, and silent at CD. Atheroembolic renal disease is an under-diagnosed cause of AKI in elderly patients. Cholesterol emboli from spontaneous/iatrogenic mobilization of atheromatous plaques in aorta or great arteries occlude small renal arteries. When the cause of AKI remains unknown, especially in patients with cardiogenic syncope or after endovascular manoeuvres, an asymptomatic renal hypoperfusion has to be suspected.

RVT may occur in renal and/or retroperitoneal cancer, peri-renal abscesses, trauma, compression or it may be related to primary renal diseases with nephrotic syndrome. Primary RVT occurs in children by dehydration and thrombocytopenia¹⁸ and in adults with nephrotic syndrome¹⁹ (Fig. 33.5). RVT rarely causes fall of GFR due to several venous anastomosis. However, in acute renal vein occlusion, collateral vessels cannot prevent acute venous congestion. This leads to an increase in kidney volume, a decrease in renal blood flow, and, subsequently, to AKI. US and CD findings of RVT are: 1) iso-echoic (recent thrombosis) or hyper-echoic organized thrombus or 2) absent or decreased venous flow with no V/t curve in the renal vein.²⁰ In primary RVT, thrombi occupy the entire vein lumen but do not deform it, while in secondary RVT renal vein appears irregular and dilated due to thrombus wall compression.²¹

POSTRENAL AKI

A single well-functioning kidney is able to preserve GFR so postrenal AKI occurs only in 1% to 10% of cases of urinary tract obstruction such as in bilateral obstruction, or in a solitary kidney with/without preexisting CKD²² (Fig. 33.6). Vesico-ureteral reflux and congenital urinary tract stenosis are the most common causes of AKI. Surgery, pregnancy, or pelvic organs cancer are the more frequent

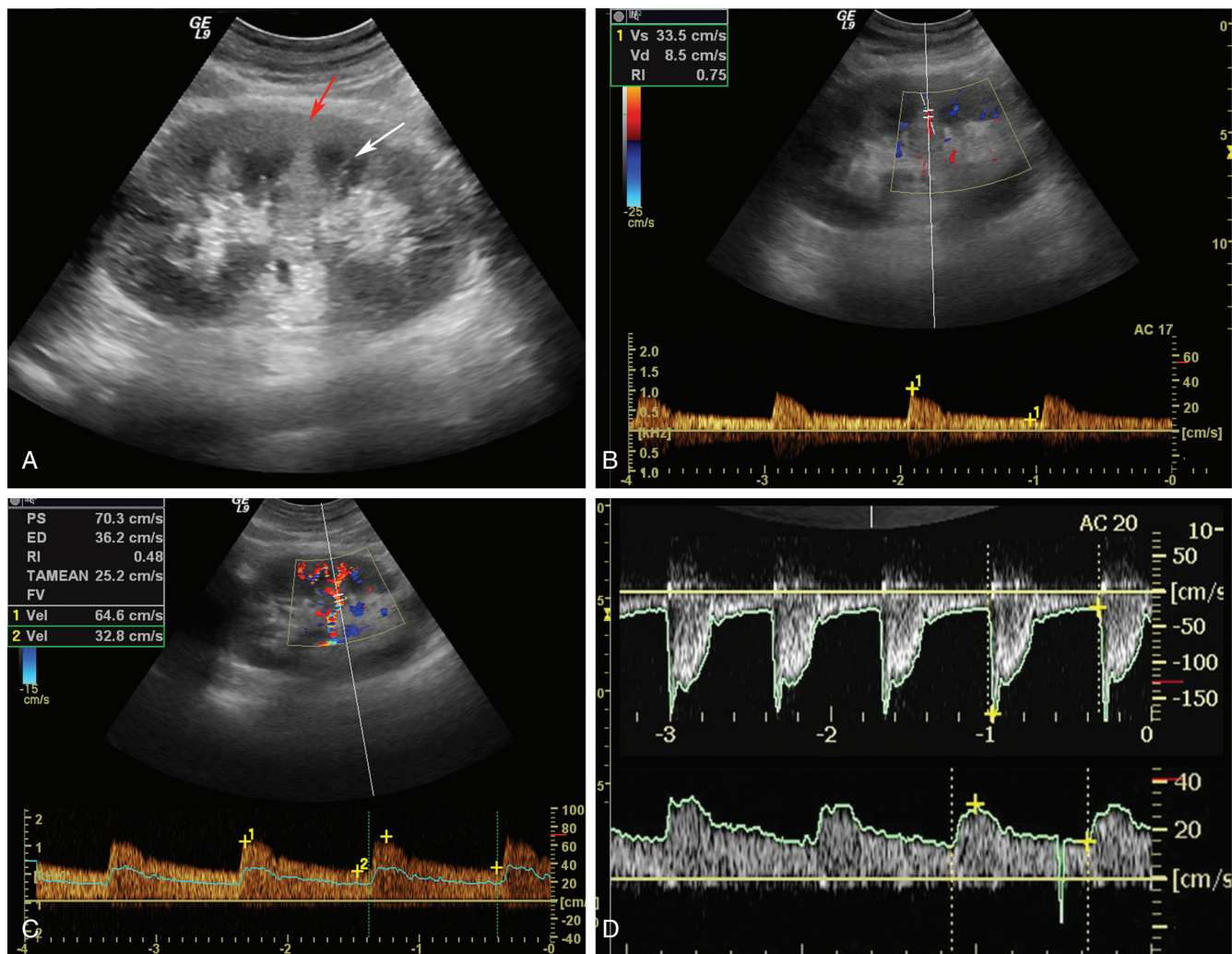


FIGURE 33.4 See also color plates. Acute tubular necrosis due to anticryptogams. Male, aged 39. Twelve hours after the abuse of anticryptogams, he was referred to a nephrologist because of oliguria and rapid increase of serum creatinine (sCr) up to 3.9 mg/dL. (A) At B-Mode ultrasound examination, both kidneys were enlarged (coronal diameter >12.5 cm), globose-shaped with a hyperechoic cortex (arrow) Ruolo del Color-Doppler nella diagnosi di trombosi primitiva della vena renale and irregular and not well distinguished pyramids. Color-Doppler sampling of right and left renal artery showed a severe reduction of diastolic velocity due to the increase of intrarenal resistances and flow redistribution. (B) Parenchymal blushing decreased and perfusion became evident only by using a low pulse repetition frequency. Color-Doppler sampling of inter-lobar arteries showed a diffuse increase of renal resistive indexes (RRI) from 0.75 to 0.81, revealing a widespread tubular damage. Patient underwent renal ultrasound and color-Doppler after 12 days from admission to the nephrology unit. At B-Mode ultrasound examination, renal morphology was unchanged, while at color-Doppler sampling of interlobar arteries, RRI returned to normal values in both the right (C) and the left kidney. The parenchymal blushing diffusely increased and the diastolic flow was present, indicating low vascular resistances (RI = 0.57-0.59). The recovery of a normal renal perfusion anticipated a moderate polyuric phase, which happened contemporarily to the recovery of renal function. (D) Doppler curves were recorded in the interlobar arteries during the acute phase and the recovery phase.

causes of postrenal AKI in young women. In elderly aged >60 years, obstruction is more frequent in male than in female due to frequency of prostate hypertrophy or cancer. US has a key role in the diagnosis of urinary obstruction.²³ However, despite its high sensitivity (>95%), detection of hydronephrosis at US does not necessarily mean obstruction, thus reducing its specificity (<70%).²³ When the excretory system is dilated, an anechoic and multiloculated fluid effusion appears into the renal sinus. Hydronephrosis shapes the upper urinary tract morphology. The renal calyces appear as multiple small anechoic rounded gaps, which are closely linked with renal parenchyma and communicate with each other. The pelvis converges into a duct with a variable diameter, and the ureter that runs along the medial profile of psoas muscle crosses the external iliac vessels and sinks

into the small pelvis. The major limitations of US in diagnosis and follow-up of obstruction are related to poor visibility of lumbar and pelvic ureter and to low specificity. In fact, there are several conditions simulating a hydronephrosis such as hyperhydration, diuretics, pregnancy, mega-calycosis. Conversely, several diseases may cause ureteral obstruction without evidence of urinary tract dilation such as retroperitoneal fibrosis, postactinic fibrosis, and lymphomatous infiltration.

Nevertheless, specificity of US increases significantly through the measurement of intrarenal RI and the visualization of ureteral jets at CD. 1) Regarding hemodynamic changes, it has been shown that RIs are significantly higher in obstructed than in non-obstructed kidneys.²⁴ During the first 12 hours after an obstruction, RIs are very high and

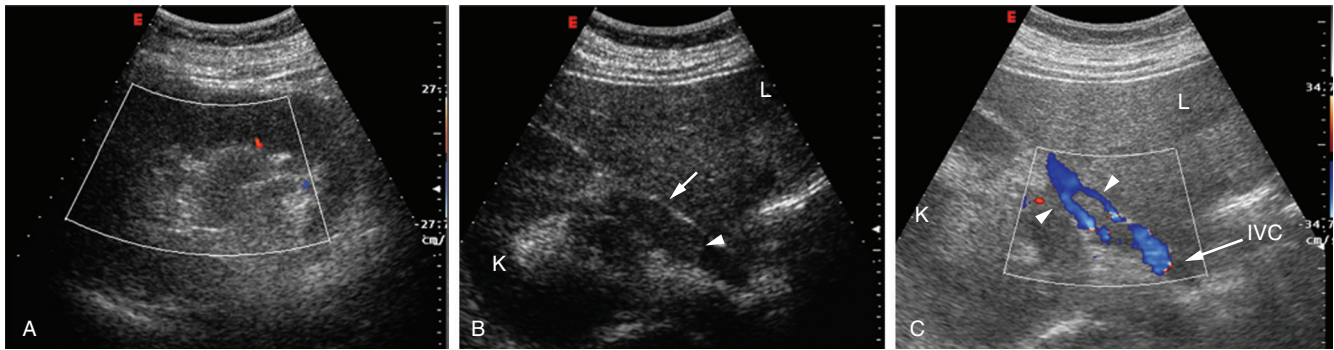


FIGURE 33.5 See also color plates. Bilateral renal vein thrombosis in a patient with nephritic syndrome secondary to focal glomerulosclerosis. Male, aged 23, with normal glomerular filtration rate (GFR) and proteinuria 12-17 g/day. Ultrasound evaluation was required after acute worsening of GFR and low back pain (serum creatinine was 3.7 mg/dl). Right kidney longitudinal diameter was 14 cm and it appeared hypoechoic, globose-shaped. Ruolo del Color-Doppler nella diagnosi di trombosi primitiva della vena renale and hypoperfused (A). Resistive indexes were 0.68. Right renal vein showed a hypoechoic material (white arrows) filling most part of the lumen (arrowhead) (B). After systemic anticoagulant therapy (C), the vein showed a partial recanalization with thin flow signals (arrowhead) around the thrombus. The progressive improvement in vessel perfusion occurred together with functional recovery. K, Kidney; L, liver; IVC, inferior vena cava.

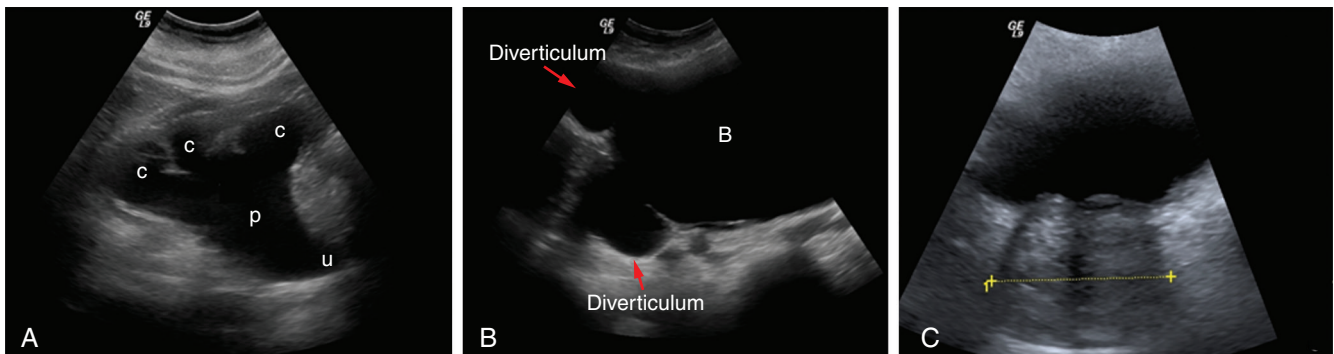


FIGURE 33.6 See also color plates. Acute kidney injury due to acute urinary tract obstruction in patient with benign prostatic hypertrophy. The patient had worsening renal function (serum creatinine 4.8 mg/dL) and anuria. (A) Massive bilateral hydronephrosis: renal calyces of both sides were dilated, corticalized, and with rounded contours. Renal pelvis and ureters were ectatic, without malformation. (B) Bladder had multiple parietal diverticula. (C) Benign prostatic hypertrophy: Transversal diameter 63 mm. c, Calyces; p, pelvis; u, ureter; b, bladder.

show a clear lateralization towards the obstruction side due to preglomerular vasoconstriction. A few hours later, RIs gradually reduce. 2) Ureteral jets represent urine flowing into the bladder from the ureter. This sign helps to establish ureter patency.²⁵ A stimulated diuresis test could be useful for the differential diagnosis in mild hydronephrosis²³ as well as an evaluation of ureteral jet and twinkling artefact in differential diagnosis of ureteral lithiasis.²⁵

(oedema, effusion in the serous cavities, lung comet tails).

4. Morphology and dynamics of inferior vena cava (IVC) and hepatic veins may be very helpful in HF to evaluate systemic overload and changes of central venous pressure.

Key Points

1. US is a multiparametric imaging technique, safe, useful, and easy to access by nephrologists and intensivists. It can be performed at bedside with considerable advantages.
2. US is the most suitable technique in clinical workup of AKI to evaluate kidney morphology and micro-circulation dynamics and to exclude an obstruction or chronic kidney disease (CKD).
3. Various parameters of systemic and pulmonary overload may be obtained with US to define clinical framework in acute or chronic heart failure (HF)

Key References

4. Meola M, Samoni S, Petrucci I, et al. Clinical Scenarios in Acute Kidney Injury: Parenchymal Acute Kidney Injury-Tubulo-Interstitial Diseases. *Contrib Nephrol.* 2016;188:39-47. doi:10.1159/000445466.
5. O'Neill WC. B-mode sonography in acute renal failure. *Nephron Clin Pract.* 2006;103:c19-c23.
6. Pozzi Mucelli R, Bertolotto M, Quaia E. Imaging techniques in acute renal failure. *Contrib Nephrol.* 2001;132:76-91.
13. Scheinfeld MH, Bilali A, Koenigsberg M. Understanding the spectral Doppler waveform of the hepatic veins in health and disease. *Radiographics.* 2009;29:2081-2098.
19. Meola M, Samoni S, Petrucci I, et al. Clinical Scenarios in Acute Kidney Injury-Parenchymal Acute Kidney Injury - Vascular Diseases. *Contrib Nephrol.* 2016;188:48-63. doi:10.1159/000445467.

A complete reference list can be found online at ExpertConsult.com.

References

1. Meola M. Malattia renale acuta. In: Meola M, ed. *Ecografia clinica in Nefrologia*. Lucca: Eureka srl; 2015:502.
2. Mehta RL, Kellum JA, Shah SV, et al; Acute Kidney Injury Network. Acute Kidney Injury Network: report of an initiative to improve outcomes in acute kidney injury. *Crit Care*. 2007;11:R31.
3. Waikar SS, Liu KD, Chertow GM. Diagnosis, epidemiology and outcomes of acute kidney injury. *Clin J Am Soc Nephrol*. 2008;3:844-861.
4. Singbartl K, Kellum JA. AKI in the ICU: definition, epidemiology, risk stratification, and outcomes. *Kidney Int*. 2012;81:819-825.
5. O'Neill WC. B-mode sonography in acute renal failure. *Nephron Clin Pract*. 2006;103:c19-c23.
6. Pozzi Mucelli R, Bertolotto M, Quaia E. Imaging techniques in acute renal failure. *Contrib Nephrol*. 2001;132:76-91.
7. Meola M. il trapianto renale. In: Meola M, ed. *Ecografia clinica in Nefrologia*. Lucca: Eureka srl; 2015:1373.
8. Quaia E, Bertolotto M. Renal parenchymal diseases: is characterization feasible with ultrasound? *Eur Radiol*. 2002;12:2006-2020.
9. Friedrich JO, Adhikari N, Herridge MS, et al. Meta-analysis: low-dose dopamine increases urine output but does not prevent renal dysfunction or death. *Ann Intern Med*. 2005;142:510-524.
10. Ronco C, Haapio M, House AA, et al. Cardiorenal syndrome. *J Am Coll Cardiol*. 2008;52:1527-1539.
11. Picano E, Frassi F, Agricola E, et al. Ultrasound lung comets: a clinically useful sign of extravascular lung water. *J Am Soc Echocardiogr*. 2006;19:356-363.
12. Rosner MH, Ronco C. Techniques for the assessment of volume status in patients with end stage renal disease. *Semin Dial*. 2014;27:538-541.
13. Scheinfeld MH, Bilali A, Koenigsberg M. Understanding the spectral Doppler waveform of the hepatic veins in health and disease. *Radiographics*. 2009;29:2081-2098.
14. Moreau R, Lebrec D. Acute renal failure in patients with cirrhosis: perspectives in the age of MELD. *Hepatology*. 2003;37:233-243.
15. Barozzi L, Valentino M, Santoro A, et al. Renal ultrasonography in critically ill patients. *Crit Care Med*. 2007;35(suppl):S198-S205.
16. Darmon M, Schortgen F, Vargas F, et al. Diagnostic accuracy of Doppler renal resistive index for reversibility of acute kidney injury in critically ill patients. *Intensive Care Med*. 2011;37:68-76.
17. Bolderman R, Oyen R, Verrijcken A, et al. Idiopathic renal infarction. *Am J Med*. 2006;119:356-359.
18. Brandão LR, Simpson EA, Lau KK. Neonatal renal vein thrombosis. *Semin Fetal Neonatal Med*. 2011;16:323-328.
19. Meola M, Samoni S, Petrucci I, et al. Clinical Scenarios in Acute Kidney Injury-Parenchymal Acute Kidney Injury - Vascular Diseases. *Contrib Nephrol*. 2016;188:48-63.
20. Biassoli E, Petrucci I, Meola M. Ruolo del Color-Doppler nella diagnosi di trombosi primitiva della vena renale. In: Meola M, ed. *Aggiornamenti di ecografia e color Doppler*. Lucca: Eureka srl; 2005:115-119.
21. Petrucci I, Biassoli E, Frangioni S, et al. La trombosi secondaria della vena renale: casi clinici e revisione della letteratura. In: Meola M, ed. *Aggiornamenti di ecografia e color Doppler*. Lucca: Eureka srl; 2005:120-124.
22. Licurse A, Kim MC, Dziura J, et al. Renal ultrasonography in the evaluation of acute kidney injury: developing a risk stratification framework. *Arch Intern Med*. 2010;170:1900-1907.
23. Meola M, Samoni S, Petrucci I, et al. Clinical Scenarios in Acute Kidney Injury: Post-Renal Acute Kidney Injury. *Contrib Nephrol*. 2016;188:64-68.
24. Pepe P, Motta L, Pennisi M, et al. Functional evaluation of the urinary tract by color-Doppler ultrasonography (CDU) in 100 patients with renal colic. *Eur J Radiol*. 2005;53:131-135.
25. Bertolotto M, Perrone R, Rimondini A. Kidney obstruction: potential use of ultrasonography and Doppler color ultrasonography. *Arch Ital Urol Androl*. 2000;72:127-134.